

# Carbon Nanotubes: Synthesis, Integration, and Properties

HONGJIE DAI\*

Department of Chemistry, Stanford University,  
Stanford, California 94305

Received January 23, 2002

## ABSTRACT

Synthesis of carbon nanotubes by chemical vapor deposition over patterned catalyst arrays leads to nanotubes grown from specific sites on surfaces. The growth directions of the nanotubes can be controlled by van der Waals self-assembly forces and applied electric fields. The patterned growth approach is feasible with discrete catalytic nanoparticles and scalable on large wafers for massive arrays of novel nanowires. Controlled synthesis of nanotubes opens up exciting opportunities in nanoscience and nanotechnology, including electrical, mechanical, and electromechanical properties and devices, chemical functionalization, surface chemistry and photochemistry, molecular sensors, and interfacing with soft biological systems.

## Introduction

Carbon nanotubes represent one of the best examples of novel nanostructures derived by bottom-up chemical synthesis approaches. Nanotubes have the simplest chemical composition and atomic bonding configuration but exhibit perhaps the most extreme diversity and richness among nanomaterials in structures and structure–property relations.<sup>1</sup> A single-walled nanotube (SWNT) is formed by rolling a sheet of graphene into a cylinder along an  $(m, n)$  lattice vector in the graphene plane (Figure 1). The  $(m, n)$  indices determine the diameter and chirality, which are key parameters of a nanotube. Depending on the chirality (the chiral angle between hexagons and the tube axis), SWNTs can be either metals or semiconductors, with band gaps that are relatively large ( $\sim 0.5$  eV for typical diameter of 1.5 nm) or small ( $\sim 10$  meV), even if they have nearly identical diameters.<sup>1</sup> For same-chirality semiconducting nanotubes, the band gap is inversely proportional to the diameter. Thus, there are infinite possibilities in the type of carbon tube “molecules”, and each nanotube could exhibit distinct physical properties.

The past decade has witnessed intensive theoretical and experimental effort toward elucidating the extreme sensitivity of the electronic properties of nanotubes to their atomic structures.<sup>2–6</sup> It has been revealed that metallic and semiconducting nanotubes exist in all materials synthesized by arc-discharge, laser ablation, and chemical vapor deposition methods. Metallic SWNTs have become model systems for investigating the rich quantum phenomena in quasi-1d solids, including single-electron

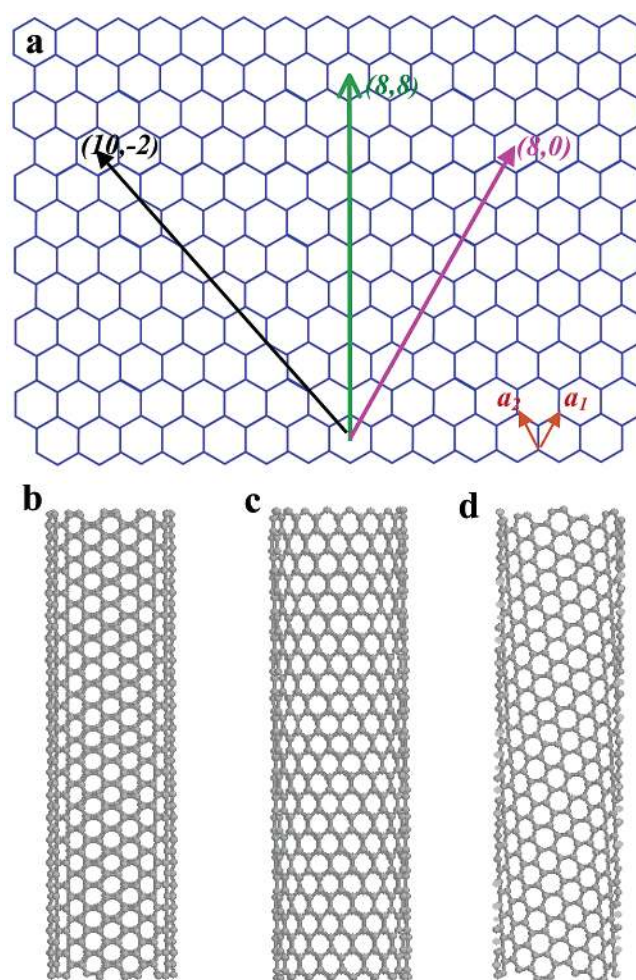


**FIGURE 1.** (a) Schematic honeycomb structure of a graphene sheet. Single-walled carbon nanotubes can be formed by folding the sheet along lattice vectors. The two basis vectors  $a_1$  and  $a_2$  are shown. Folding of the  $(8, 8)$ ,  $(8, 0)$ , and  $(10, -2)$  vectors lead to armchair (b), zigzag (c), and chiral (d) tubes, respectively.

charging, Luttinger liquid, weak localization, ballistic transport, and quantum interference.<sup>2–4,7,8</sup> On the other hand, semiconducting nanotubes have been exploited as novel building blocks for nanoelectronics, including transistors and logic, memory, and sensory devices.<sup>2–6</sup>

Nanotube characterization and device explorations have been greatly facilitated by progress in nanotube synthesis over the years. At the same time, many aspects of basic research and practical application requirements have been driving and motivating synthetic methods for better and more homogeneous materials. This complementary cycle continues, and it is now at a time when nanotube synthesis has evolved from enabling growth into consciously controlling the growth. While the extreme sensitivity of nanotube structure–property relations has led to rich science and promises a wide range of applications, it poses a significant challenge to chemical synthesis in controlling the nanotube diameter and chirality. Understanding how to synthesize nanotubes with predictable

Hongjie Dai was born in Shaoyang, Hunan, P. R. China, in 1966. He received his B.S. from Tsinghua University in 1989, his M.S. from Columbia University in 1991, and his Ph.D. from Harvard University with Charles Lieber in 1994. After postdoctoral work with Richard E. Smalley at Rice University, he joined the faculty of the Chemistry Department at Stanford University in 1997.

\* E-mail: hdai1@stanford.edu.

properties essentially requires exquisite control of atomic arrangement along the tubes, which is an ultimate task for chemists in the nanotube field.

Arc-discharge, laser ablation, and chemical vapor deposition have been the three main methods used for carbon nanotube synthesis.<sup>6</sup> The first two employ solid-state carbon precursors to provide carbon sources needed for nanotube growth and involve carbon vaporization at high temperatures (thousands of degrees Celsius). These methods are well established in producing high-quality and nearly perfect nanotube structures, despite large amounts of byproducts associated with them. Chemical vapor deposition (CVD) utilizes hydrocarbon gases as sources for carbon atoms and metal catalyst particles as “seeds” for nanotube growth that takes place at relatively lower temperatures (500–1000 °C).<sup>6</sup> For SWNTs, none of the three synthesis methods has yielded bulk materials with homogeneous diameters and chirality thus far. Nonetheless, arc-discharge and laser ablation techniques have produced SWNTs with impressively narrow diameter distributions averaging  $\sim 1.4$  nm. CVD methods have come a long way from producing carbon fibers, filaments, and multiwalled carbon nanotubes to the synthesis of SWNTs<sup>6,9–14</sup> with high crystallinity and perfection comparable to those of arc<sup>15</sup> and laser<sup>16</sup> materials, as revealed by electrical transport and microscopy and spectroscopy measurements.

This Account presents our up-to-date research on controlling the growth of carbon nanotubes by CVD approaches. While arc-discharge and laser ablation methods produce only tangled nanotubes mixed randomly with byproducts, we illustrate that site-selective CVD synthesis on catalytic patterned substrates grows nanotube arrays at controllable locations and with desired orientations on surfaces. We further show successful chemical vapor deposition of SWNTs on preformed discrete catalytic nanoparticles. The results suggest that understanding the chemistry involved in the growth and controlling the catalytic nanoparticles could eventually allow for the control of the diameter and chirality of nanotubes. We also review elucidations of the interplay of electrical, mechanical, and chemical properties of nanotubes as facilitated by our progress in controlled materials synthesis. Implications of nanotube functionalization, molecular sensors, and interfacing with biological molecules are discussed.

## Patterned Growth of Nanotubes

Carbon nanotube synthesis by CVD involves heating a catalyst material in a furnace and flowing a hydrocarbon gas through the tube reactor for a period of time. The catalytic species are transition-metal nanoparticles typically supported on high surface area materials (alumina) materials.<sup>6</sup> Simplistically, the catalyst particles serve as seeds to nucleate the growth of nanotubes. We have developed patterned growth approaches to obtain organized nanotube structures. The idea is to position catalyst in arrayed fashions for the growth of nanotubes from

specific catalytic sites on surfaces.<sup>9</sup> We have carried out such patterned growth for both multiwalled and single-walled nanotubes, exploited ways including self-assembly and active electric field control to manipulate the orientation of nanotubes, and pursued several generations of catalysts ranging from powdery supported catalyst to discrete catalytic nanoparticles. These works have led to ordered nanotube arrays or networks formed at the synthesis stage of nanotubes.

**(a) Ordered Arrays of Multiwalled Nanotubes—Self-Assembly by Intratube van der Waals Interactions.** Our earlier work has demonstrated the synthesis of regular arrays of ordered towers consisting of multiwalled nanotubes (MWNTs) by CVD growth (700 °C; carbon source,  $C_2H_4$ ; alumina-supported iron catalyst) on porous silicon or silicon substrates patterned with iron particles in square regions (Figure 2a).<sup>17</sup> The nanotubes within each tower are well aligned along the direction perpendicular to the substrate surface. The alignment is a result of nanotubes grown from closely spaced catalyst particles in each square self-assembling into rigid bundle structures due to strong intratube van der Waals binding interactions. The rigidity of the assembly allows the nanotubes to self-orient and grow perpendicular to the substrate. The arrayed nanotubes exhibit excellent characteristics in electron field emission, opening up the possibility of spatially defined massive field emitter arrays derived by simple chemical routes for flat panel display applications.<sup>17</sup>

**(b) Ordered Networks of Suspended Single-Walled Nanotubes—Self-Assembly by van der Waals Interactions with Substrates.** We have synthesized suspended SWNT networks with well-defined orientations on substrates containing lithographically patterned silicon posts.<sup>18,19</sup> Contact printing is used to transfer catalyst materials onto the tops of pillars selectively, and CVD (900 °C; carbon source,  $CH_4$ ; supported iron catalyst derived by a template method from liquid precursors) on the substrates leads to suspended SWNTs forming nearly ordered networks with the nanotube orientations directed by the pattern of the silicon posts (Figure 2b–d). The mechanism for nanotube self-orienting in this case is due to van der Waals interactions between nanotubes and the silicon posts. The nanotubes grown from the posts float and wave in the gas until they are fixed by nearby posts. The suspended nanotube networks are difficult to obtain otherwise by, e.g., postgrowth assembly with arc- or laser-grown materials and are useful for building novel nanoelectromechanical devices (NEMs).

**(c) Electric-Field-Directed Nanotube Growth.** We recently have exploited electric fields to actively control the growth directions of SWNTs.<sup>20</sup> Highly aligned suspended SWNTs are grown under electric fields on the order of  $\sim 1$  V/ $\mu m$  (Figure 2e). The alignment effect originates from the high polarizability of SWNTs. The induced dipole moment for a  $\sim 10$   $\mu m$  SWNT in a 1 V/ $\mu m$  electric field is about  $10^6$  D, leading to a large aligning torque that directs the nanotube parallel to the electric field. Importantly, the electric field alignment effect is stable against thermal fluctuations at the growth temperature and against gas

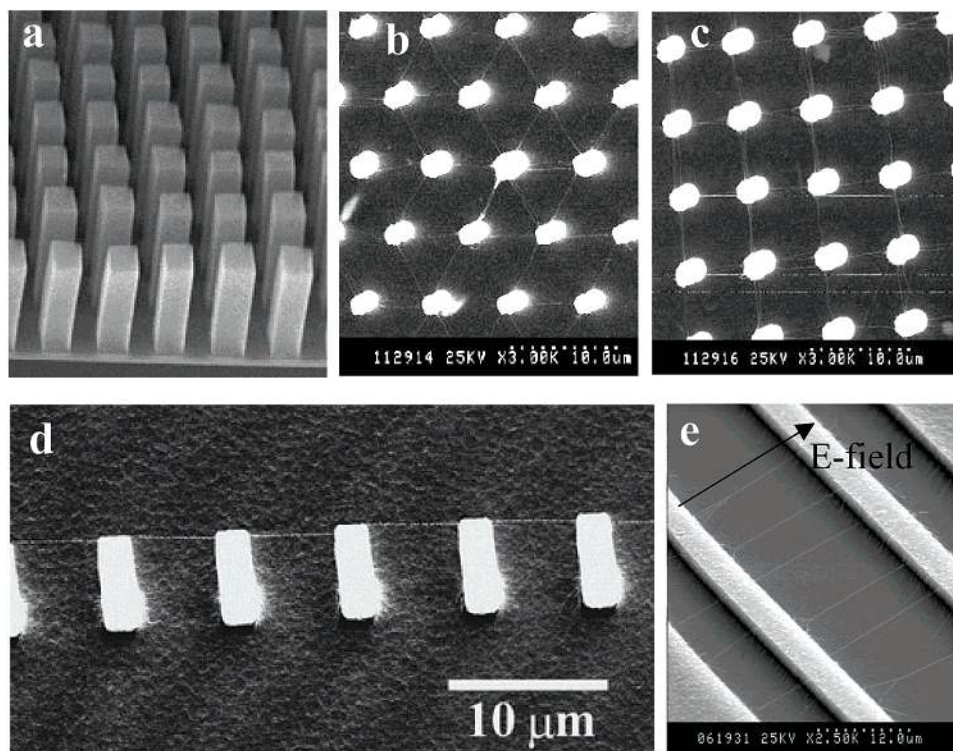


**FIGURE 2.** Ordered carbon nanotube structures obtained by direct chemical vapor deposition synthesis. (a) An SEM image of self-oriented MWNT arrays. Each tower-like structure is formed by many closely packed multiwalled nanotubes. Nanotubes in each tower are oriented perpendicular to the substrate. (b) SEM top view of a hexagonal network of SWNTs (line-like structures) suspended on top of silicon posts (bright dots). (c) SEM top view of a square network of suspended SWNTs. (d) Side view of a suspended SWNT power line on silicon posts (bright). (e) SWNTs suspended by silicon structures (bright regions). The nanotubes are aligned along the electric field direction.

flow randomization effects. Manipulation by applied fields during nanotube synthesis is highly promising for further exploration of both suspended molecular wires and complex nanotube fabric structures on flat substrates.

**(d) From Powdery Catalyst to Isolated Catalytic Nanoparticles—Toward Nanotube Structural Control and Microscopic Understanding of Growth.** Supported catalyst typically used for SWNTs growth consists of powdery support with attached metal nanoparticles that are difficult to characterize by microscopy. As a result, the size of the catalytic nanoparticles is hard to control. Recently, we have pursued isolated iron nanoparticles for the synthesis of SWNTs by CVD.<sup>21,22</sup> Controllable numbers of  $\text{Fe}^{3+}$  are placed into the cores of apoferritin to afford stable solutions of artificial ferritin that can be subsequently deposited onto flat substrates. Calcination in air leads to discrete  $\text{Fe}_2\text{O}_3$  nanoparticles with average diameter  $\sim 1.5$  nm, as characterized by atomic force microscopy (AFM) and transmission electron microscopy (TEM). AFM and TEM have revealed successful growth of SWNTs from the isolated nanoparticles (Figure 3). Further, synthesis of SWNTs directly on TEM grids has allowed us to clearly reveal the nanoparticle–nanotube relationship (Figure 3a–f).

Our data provide evidence that, first, the diameters of SWNTs are closely determined by the diameters of catalytic particles and second, TEM imaging of both ends of isolated SWNTs (Figure 3a,d,e) points to the so-called base-growth model of SWNTs in our CVD process. That is, the catalytic nanoparticle remains on the supporting

substrate, and a nanotube grows out from the particle with a dome-closed end (Figure 3g). The CVD reaction process then involves carbon atoms, decomposed from methane, absorbing into the anchored nanoparticle on the substrate to form a carbon–iron solid-state solution. As supersaturation occurs, carbon atoms precipitate out from the particle, leading to the growth of a nanotube (Figure 3g). This growth model is in contrast with the tip-growth model, in which catalyst particles lift off from the substrate during growth.

Synthesis with controllable catalyst, although still in its early stage,<sup>21–23</sup> has led to important clues to the nanotube growth chemistry, mechanism, and structural control. Future work will include determining the nature of SWNTs (metal vs semiconductor) grown from individual particles, experimentally and theoretically investigating how a seed particle determines the nanotube chirality, and obtaining highly monodispersed nanoparticles at the 1 or 2 nm level. We have also carried out patterned growth with ferritin particles placed in micrometer-scale squares on surfaces (Figure 3h). New lithographic approaches capable of 10 nm features are required to enable catalytic patterning of individual nanoparticles. Meeting these challenges will be extremely rewarding, leading to (1) rational routes to nanotube diameter and chirality control and (2) dense and ordered networks of nanotubes with predictable metallic or semiconducting electronic properties.

**(e) Scalability of Patterned Growth.** Assembly of nanotube arrays must be scaled-up on large substrates for various practical applications. To this end, we have



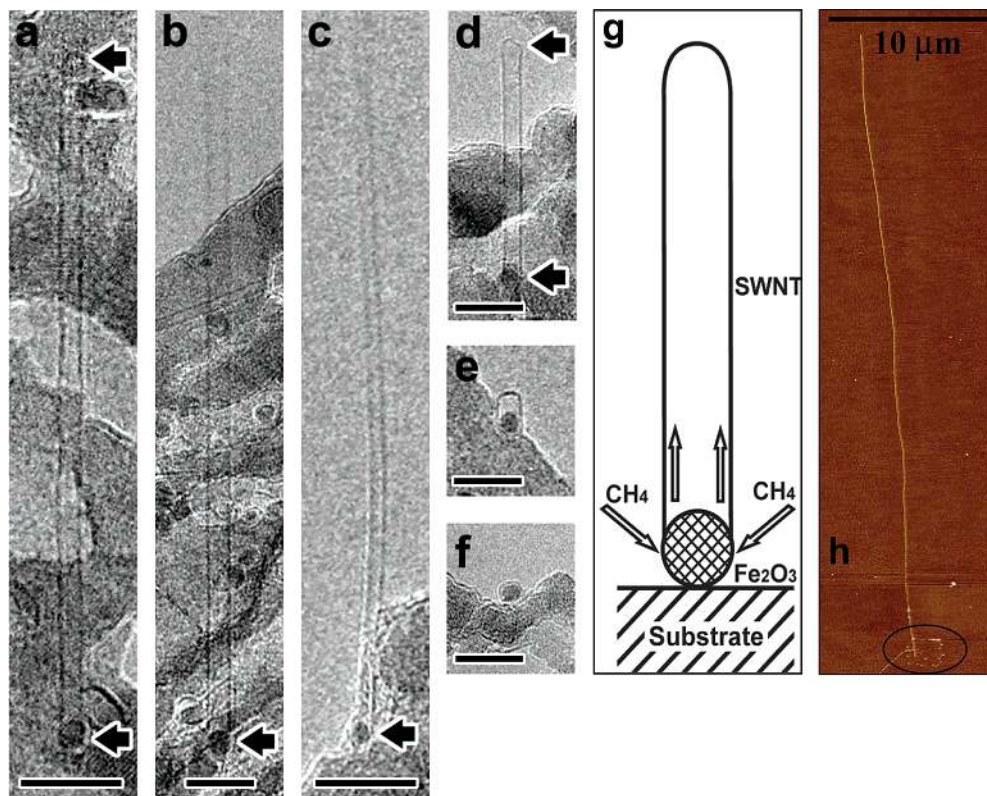


**FIGURE 3.** (a–f) TEM images of SWNTs grown from discrete nanoparticles, showing particle–nanotube relationships. Scale bars: 10 nm. (a–d) SWNTs grown from discrete nanoparticles (dark dots at the bottom of the images). The arrows point to the ends of the nanotubes. The ends extending out of the membrane in (b) and (c) are not imaged due to thermal vibration. The background roughness reflects the TEM grid morphology. (e) Image of an ultrashort ( $\sim 4$  nm) nanotube capsule grown from a  $\sim 2$  nm nanoparticle. (f) Image of a nanoparticle surrounded by a single graphitic shell. (g) A schematic model for nanotube growth. (h) AFM image of a  $50\ \mu\text{m}$  long SWNT grown from nanoparticles patterned into the circled region.

explored patterned growth of SWNTs on full 4-in. SiO<sub>2</sub>/Si wafers.<sup>24</sup> We have patterned micrometer-sized catalyst islands with high uniformity over entire wafers by a photolithography approach (Figure 4a). We have also investigated how the gas flow rates (CH<sub>4</sub> and H<sub>2</sub> co-flow) affect the growth of SWNTs. This aspect has not been systematically studied in our earlier synthesis work. We have identified that, for relatively low CH<sub>4</sub> flow rates, the CVD process is ultrasensitive to the amount of H<sub>2</sub> co-flow, undergoing pyrolysis, growth, and inactive reaction regimes with increased H<sub>2</sub> addition. This understanding has enabled us to grow high-quality SWNTs (Figure 4b) from massive arrays of well-defined surface sites on full 4-in. wafers.<sup>24</sup>

### Electrical Properties and Interplay with Mechanical and Chemical Properties

Patterned growth of carbon nanotubes on substrates has allowed for convenient, simple, and controlled integration of nanotubes into various device structures for elucidating the properties of individual molecular wires. With these devices, we have carried out electron transport measurements of semiconducting, quasi-metallic, and metallic SWNTs grown by CVD. Suspended nanotubes have also been integrated into addressable structures for mechanical and electromechanical characterization.

**(a) Electrical Properties of Nanotubes.** We have revealed by transport measurements (Figure 5a) that the majority of individual SWNTs synthesized by CVD on supported catalyst are semiconducting in nature. This type of nanotube exhibits field effect transistor (FET) behavior at room temperature and has been intensively explored in recent years for nanoelectronics devices, including transistors and logic devices.<sup>3,25–29</sup> The as-grown semiconducting SWNTs are hole-doped p-type FETs with hole depletion and diminished conductance (from typically 100 k $\Omega$  to 1 M $\Omega$ ) by positive gate voltages (Figure 5b). It is now established that molecular oxygen adsorbed on the nanotubes is responsible for hole doping of SWNTs.<sup>30–33</sup> Removal of O<sub>2</sub> can lead to nearly intrinsic semiconducting behavior (Figure 5b inset).<sup>33</sup> More and more investigations are revealing that, although carbon nanotubes are highly robust and inert structures, their electrical properties are extremely sensitive to charge transfer and chemical doping effects by various molecules.

The second type of observed SWNTs synthesized by CVD appears to be quasi-metallic with small band gaps on the order of 10 meV.<sup>34</sup> These nanotubes are not as sensitive as semiconducting SWNTs to electrostatic doping by gate voltages but exhibit a conductance dip associated with the small band gap. These nanotubes correspond to a class of non-armchair SWNTs, and the origin of the band

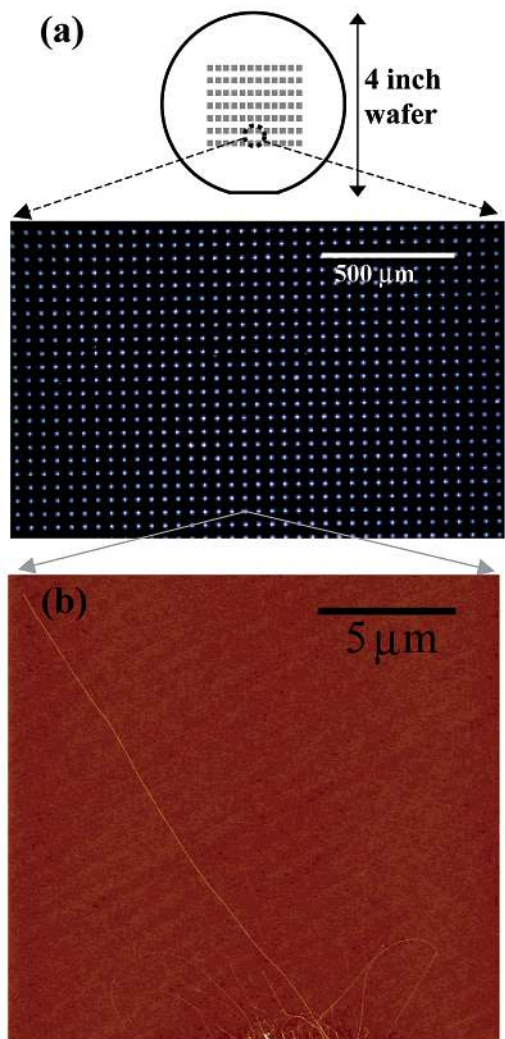


**FIGURE 4.** Wafer scale patterned nanotube synthesis. (a) An optical image showing patterned catalyst islands (bright dots). (b) AFM image of SWNTs grown and emanating from one of the catalyst islands on the wafer.

gap is slight  $sp^2$  to  $sp^3$  hybridization due to the nonflat nature of the hexagons on the tube walls.<sup>35,36</sup> Temperature-dependent measurements for some of the quasi-metallic-like SWNTs (room-temperature resistance  $\sim 10$ – $20$  k $\Omega$ ) reveals increased electrical conductance at low temperatures, reaching the  $4e^2/h = 2G_0$  quantum conductance (6.45 k $\Omega$  in resistance) limit at  $\sim 1.5$  K (Figure 5c). Quantum interference effects have also been observed.<sup>8</sup> The results suggest that (1) phonon is one of the fundamental scattering mechanisms in SWNTs at room temperature, (2) excellent ohmic contacts can be made to nanotubes with transmission probability  $T \approx 1$ , and (3) electron transport is highly phase coherent and ballistic in nanotubes at low temperatures.<sup>8</sup>

Truly metallic armchair SWNTs are rare in our CVD-grown nanotubes. The conductance of this type of nanotube is the least sensitive to gate voltages. With highly transparent ohmic contacts to these nanotubes, we have observed near  $4e^2/h$  quantum conductance in SWNTs as long as  $4 \mu\text{m}$  at low temperatures (J. Kong and H. Dai, unpublished results), suggesting a long mean free path

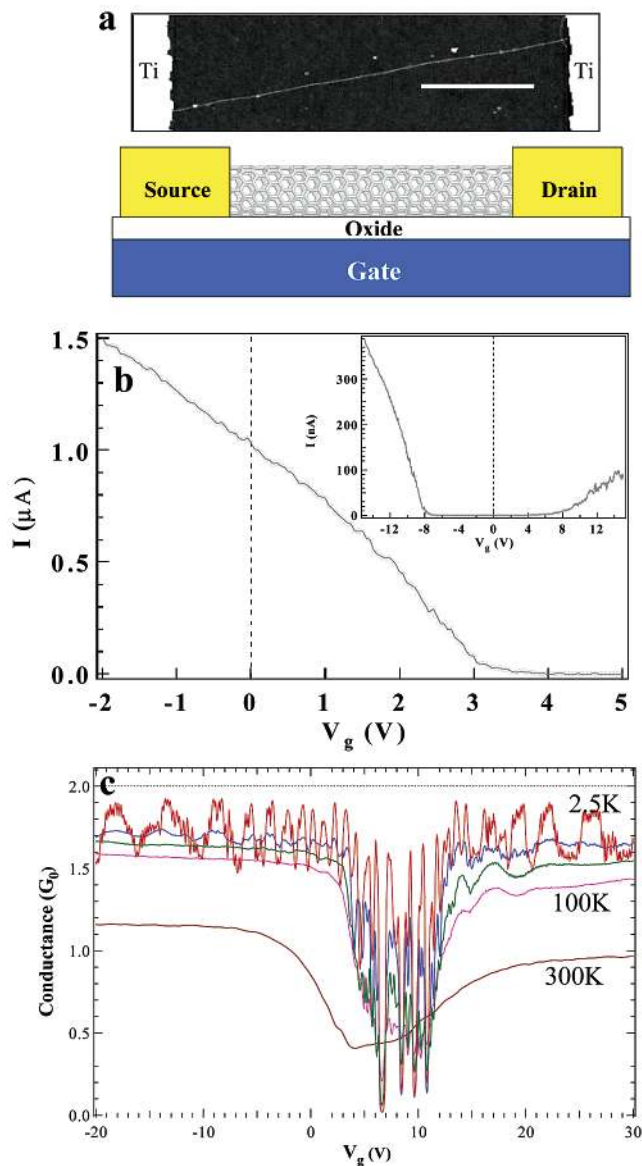


**FIGURE 5.** Electrical properties of individual nanotubes. (a) AFM image of a SWNT contacted by two Ti electrodes and a schematic cross-section view of the device. Scale bar:  $1 \mu\text{m}$ . A gate voltage ( $V_g$ ) can be applied to electrostatically couple to the nanotube and shift the Fermi level. (b)  $I$ – $V_g$  curve for a typical as-made semiconducting SWNT showing p-type FET characteristics. Inset: The p-type FET evolves into a nearly intrinsic semiconductor after removal of surface-adsorbed oxygen. (c) Conductance  $G$  (in units of quantum conductance,  $G_0 = 2e^2/h$ ) vs  $V_g$  (Fermi energy) for a quasi-metallic SWNT at various temperatures. The conductance approaches the theoretical limit  $2G_0$  at low temperatures, with conductance fluctuations due to quantum resonance effects.

for ballistic electron transport in high-quality/perfection CVD-grown SWNTs.

**(b) Nanotube Electromechanical Properties and Devices.** Patterned growth has been used to synthesize suspended SWNTs across trenches with the nanotubes wired up electrically with relative ease.<sup>37</sup> We have manipulated a suspended nanotube by using an AFM tip while monitoring its electrical conductance (Figure 6a,b). By so doing, we are able to address how mechanical deformation affects the electrical properties of carbon

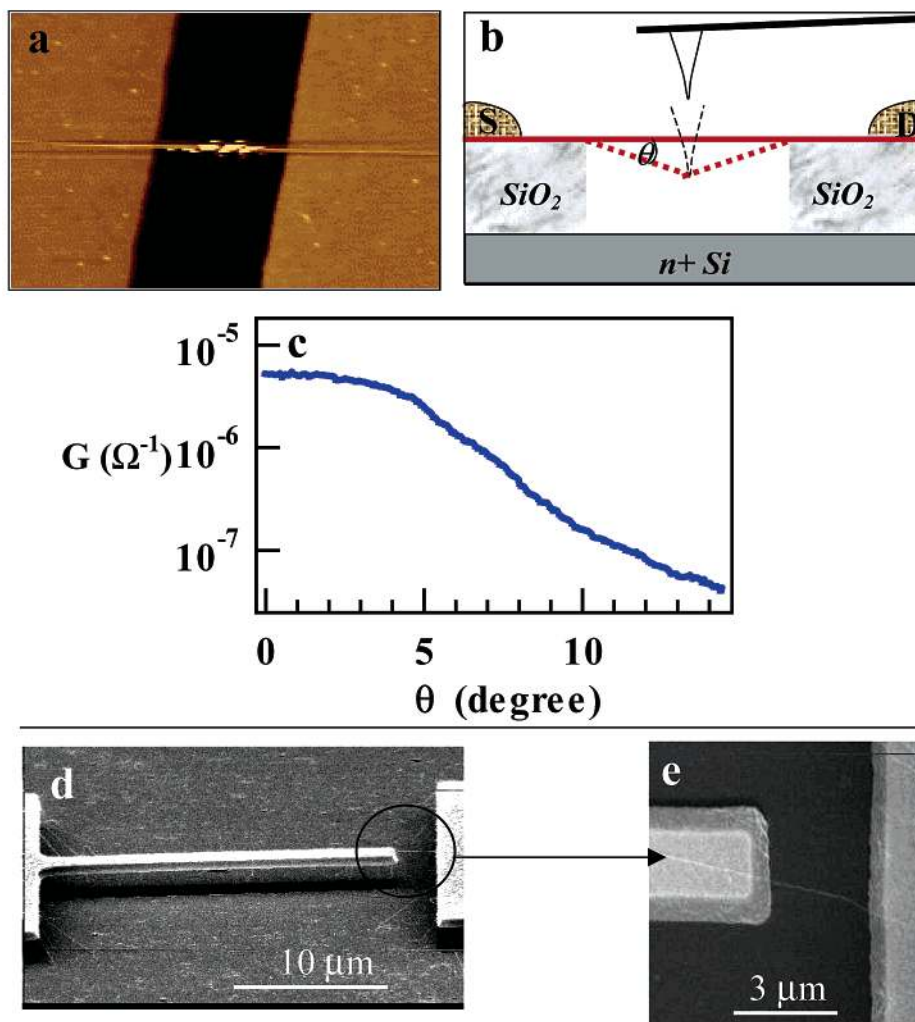


**FIGURE 6.** Nanoelectromechanics of suspended nanotubes. (a) AFM image of a suspended SWNT over a trench (dark region,  $\sim 500$  nm wide). (b) Experimental scheme for measuring the electromechanical property of the nanotube. The suspended nanotube is pushed by an AFM tip, while the conductance of the nanotube between the source (S) and drain (D) electrodes is monitored. (c) Conductance  $G$  of the nanotube vs bending angle. (d,e) SEM images showing a suspended nanotube bridging a micromechanical Si beam and a Si terrace.

nanotubes, a question important to potential nanoelectromechanical (NEM) devices.

We have measured conductance vs strain and bending angle of individual SWNTs and found a 2 orders of magnitude conductance decrease at a  $14^\circ$  bending angle and 3% strain (Figure 6c). The electrical and mechanical changes are fully reversible, suggesting potential nanowire-based electromechanical transducers.<sup>37</sup> The electromechanical behavior is rationalized by molecular dynamics simulation and conductance calculations. Large local structural distortion of the nanotube caused by mechanical actions of the AFM tip leads to carbon atoms in  $sp^3$ -like bonding configurations, which is responsible for electron localization and significant local barriers for electron transport through the nanotube.<sup>37,38</sup>

We are extending our patterned growth approaches to obtaining new types of suspended nanotube NEMs structures for basic characterization and potential devices. Suspended SWNTs have been integrated with silicon-based micromechanical structures, as shown in Figure 6, with SEM images of suspended SWNTs grown on a suspended silicon beam and bridging a terrace (Figure

6d,e). Along this line, a wide range of nanotube-based NEMs structures are obtainable for exploring pure stretching, twisting of single nanowires, and their high-frequency resonance characteristics. Functional NEMs switches and memory devices can also be envisioned. Controlled and deterministic synthesis of nanotubes will continue to open exciting and new possibilities of novel nanostructures and devices.

### Interactions with Chemical Species—From Small Molecules to Polymers

Single-walled carbon nanotubes are typically chemically inert. Covalent attachment of molecular species to fully  $sp^2$ -bonded carbon atoms on the nanotube sidewalls proves to be difficult. Adsorbing molecules to nanotubes via noncovalent forces, however, turns out to be facile and has important consequences to their physical properties and potential applications.

**(a) Molecular Adsorption and Photodesorption.** The first sign of molecular adsorption on SWNTs was noticed during electrical transport measurements as the resistance



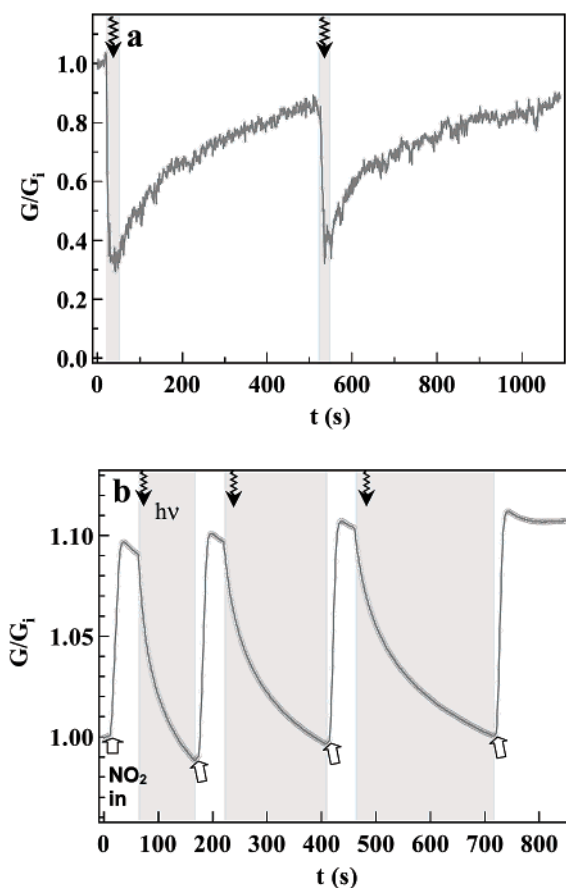


**FIGURE 7.** Molecular adsorption, photodesorption, and reversible chemical sensors. (a) Normalized conductance of an individual semiconducting SWNT during  $\text{O}_2$  desorption caused by UV illumination (shaded time periods) and  $\text{O}_2$  re-adsorption after turning off the UV. (b) Conductance response of an ensemble of SWNTs to  $\text{NO}_2$  adsorption and photodesorption (during shaded time periods) cycles. The wide arrows point to the times when  $\text{NO}_2$  is introduced into the measurement chamber and adsorbs onto SWNTs.

of semiconducting SWNTs tended to change in a vacuum versus that in air. We have systematically measured the electrical properties of SWNTs in various chemical environments and revealed various small gas molecules adsorbing onto SWNTs and undergoing charge transfer.<sup>30</sup> As a result, semiconducting SWNTs exposed to ppm levels of  $\text{NO}_2$  exhibit conductance increases by up to 3 orders of magnitude in a few seconds. When the SWNTs are exposed to  $\text{NH}_3$ , the conductance of the nanotube can decrease by up to 2 orders of magnitude.<sup>30</sup> Collins and co-workers have found similar high sensitivity to  $\text{O}_2$  adsorption.<sup>31</sup> These results have suggested nanotubes as miniature chemical sensors with high sensitivity at room temperature.

$\text{NO}_2$  and  $\text{O}_2$  on SWNTs are strongly physisorbed and do not desorb at significant rates at room temperature.  $\text{NH}_3$  is weakly physisorbed on nanotubes and can be removed by simple pumping in a vacuum. Density functional theory (DFT) calculations reveal that  $\text{NO}_2$  binds to a nanotube with an energy on the order of  $\sim 0.4$  eV<sup>39</sup> to  $0.9$  eV<sup>30,40</sup> and withdraws  $\sim e/10$  from the nanotube.  $\text{O}_2$  binds to a nanotube with  $\sim 0.25$  eV energy and  $\sim e/10$  charge-withdraw from the tube.<sup>41</sup> However, DFT calcula-

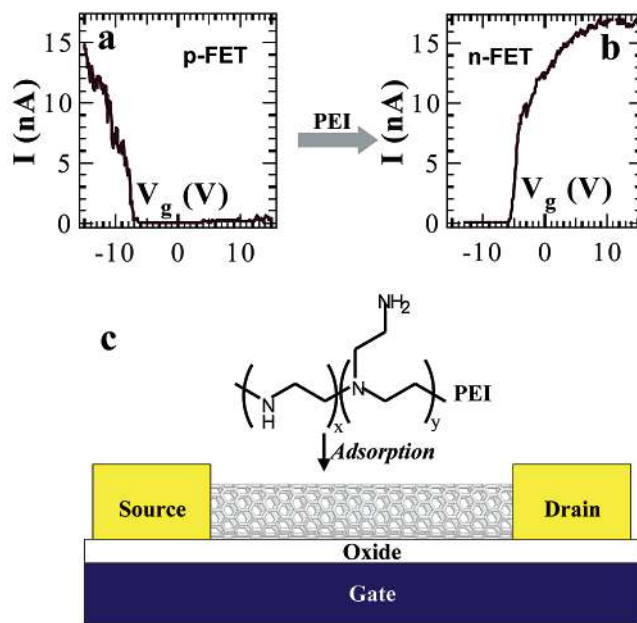


**FIGURE 8.** Polymer functionalization for air-stable n-type nanotube FET. (a) Current ( $I$ ) vs gate characteristics of an as-made semiconducting SWNT showing p-type FET behavior. (b) The nanotube evolves into an n-type FET after adsorption of PEI, schematically shown in (c).

tion does not reveal any significant binding of  $\text{NH}_3$  on nanotubes, and  $\text{NH}_3$  appears to be weakly adsorbed on nanotubes by van der Waals interactions. Despite very small charge transfer,  $\text{NH}_3$  adsorption does cause appreciable changes to the electrical property of SWNTs observed experimentally, suggesting the extreme sensitivity of SWNTs to chemical gating effects.

We have recently discovered photoinduced molecular desorption from SWNTs.<sup>33</sup> Desorption of molecules from SWNTs can certainly be achieved by heating nanotubes to high temperatures ( $\sim 200$  °C).<sup>31,32</sup> Ultraviolet (UV, 250 nm) light illumination at low photon flux causes rapid molecular desorption from SWNTs at room temperature. Figure 7a shows photodesorption of  $\text{O}_2$  and thus lowered hole-carriers in a nanotube, as signaled by the rapid electrical conductance decrease upon UV illumination. Upon turning off the UV, conductance recovery occurs due to  $\text{O}_2$  re-adsorption (Figure 7a). The photodesorption phenomenon is found to be generic to various molecules (Figure 7b) preadsorbed onto nanotubes.<sup>33</sup>

Wavelength-dependent measurements<sup>33</sup> reveal that photodesorption is due to electronic excitation of nanotubes and is a nonthermal process. Electronic excitations of  $\pi$ -plasmons in SWNTs by UV leads to electron/hole pairs via Landau damping.<sup>42</sup> We have suggested that the electrons or holes generated may attach to adsorbed molecular species, which is responsible for the observed molecular desorption. The photodesorption cross section is estimated to be  $\sigma \approx 1.4 \times 10^{-17} \text{ cm}^2$  at 250 nm for  $\text{O}_2$ .<sup>33</sup>

Our results illustrate that surface chemistry and photochemistry issues are critical to the properties and applications of molecular-scale wires that have ultrahigh surface area, with every atom on the surface. Surface

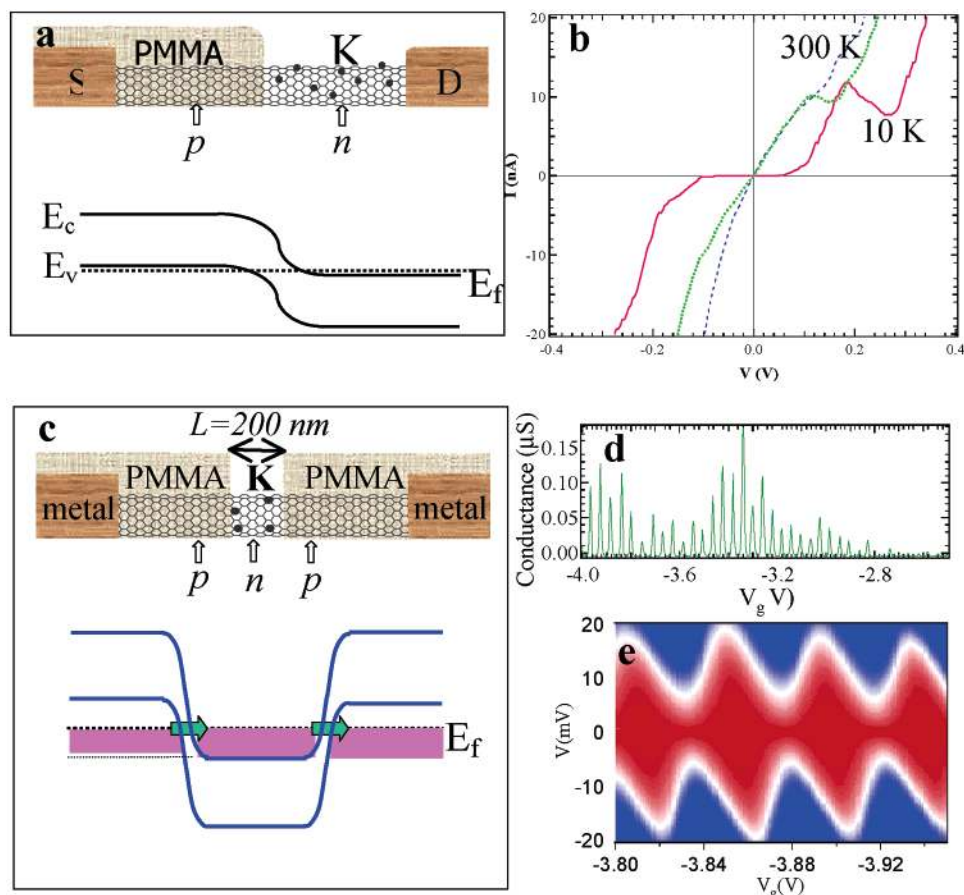


**FIGURE 9.** Chemical profiling of individual nanotubes. (a) Schematic structure and band diagram for a p–n junction formed on a nanotube. (b) Current–voltage ( $I$ – $V$ ) characteristics of the sample showing negative differential conductance at low temperatures. (c) Schematic structure and band ( $E_c$ ,  $E_v$ , and  $E_f$  are conduction band, valence band, and Fermi level, respectively) diagram for two p–n junctions formed on a nanotube. (d) Periodic conductance oscillations vs gate voltage corresponding to single-electron transport. (e) Coulomb diamonds related to single-electron transport. The diamonds enclose regions with low conductance. The number of electrons in the quantum dot changes by 1 between adjacent diamonds.

science can be elucidated at the single-wire level by using electrical/chemical properties of nanotubes as probes.

**(b) Polymer Doping.** Controlling the type of charge carriers (electron or hole) is critical to conventional n-type or p-type FETs. By the same token, both p- and n-type FETs based on SWNTs are highly desired for potential nanoelectronics. However, the classical alkali metal n-dopants for carbon systems readily oxidize and are undesirable for practical nanotube n-FETs. We have carried out functionalization of SWNTs by an amine-rich polymer, polyethyleneimine (PEI), and obtained n-type FETs that are stable in air.<sup>43</sup> An as-made p-type semiconducting SWNT due to adsorbed  $O_2$  readily reverts to an n-type FET after functionalization by PEI (Figure 8). Analysis shows that the adsorbed PEI donates approximately 1 electron to every 1000 carbon atoms on the nanotube.<sup>43</sup> Hence, instead of complete ionization of alkali, partial donating or withdrawing functional groups on organic materials can be used to dope and manipulate the charge carried in molecular wires, which may prove useful for nanoelectronics applications.

**(c) Chemical Profiling of a Single Nanotube.** We have shown that doping a nanotube with a controlled chemical

dopant profile along its length leads to interesting quantum phenomena.<sup>44–46</sup> Compared to the molecular-scale diameters (1–2 nm), the lengths of SWNTs are mesoscopic or macroscopic (1–100  $\mu m$ ) and have ample room to form nanometer junctions. We have masked half of a SWNT by polymer and doped the other half by potassium to form an intratube p–n junction (Figure 9a) that exhibits negative differential conductance (NDC) at low temperatures (Figure 9b).<sup>44</sup> NDC arises due to quantum tunneling across degenerately doped semiconducting p–n junctions, known in conventional Esaki diodes. Nondegenerate intratube p–n junctions have been formed on SWNTs by organic amine doping, leading to excellent intratube electrical rectifiers.<sup>45</sup>

We have extended the scheme to chemically profile a nanotube containing two p–n–p junctions (Figure 9c).<sup>46</sup> Electron transport measurements reveal that the nanotube section between the two chemically formed junctions defines a small ( $\sim 200$  nm long) quantum dot on a micrometers-long nanotube. The small dot on the long tube exhibits clear single-electron charging phenomenon (Figure 9b),<sup>47</sup> as a result of small structural dimensions and hence low capacitance and high charging energy



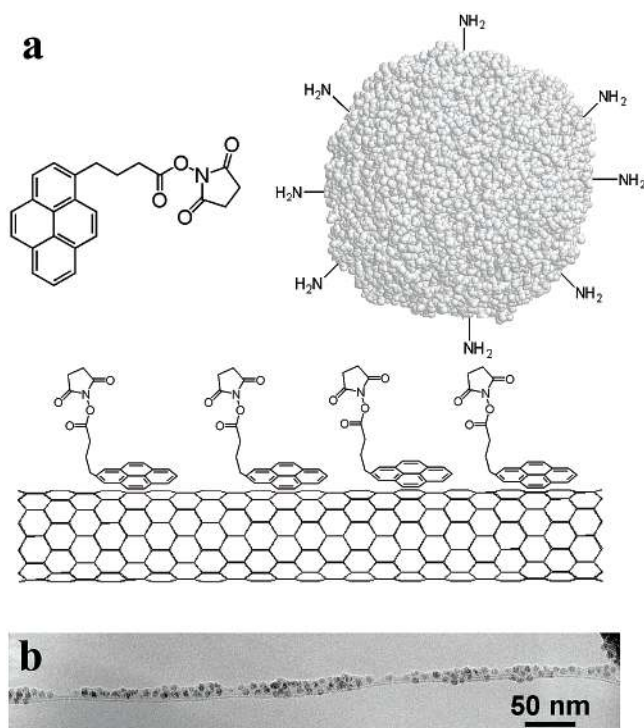


**FIGURE 10.** (a) Scheme for noncovalent functionalization of the sidewalls of nanotubes for protein immobilization. (b) A TEM image showing ferritin immobilized on a suspended nanotube by using the scheme in (a).

( $> k_B T$ ) for the “dot”. Controlled chemical doping can hence lead to interesting quantum phenomena and devices confined along the length of a nanotube.

## Functionalization and Interfacing with Biological Systems

Functionalization is an important aspect of the chemistry of nanotube “macromolecules”.<sup>48–52</sup> As mentioned, however, covalent sidewall functionalization of nanotubes from  $sp^2$  to  $sp^3$  structure is both difficult and undesired because of the loss of conjugation.<sup>49</sup> Alternatively, it is possible to functionalize SWNTs noncovalently<sup>50–52</sup> to preserve the  $sp^2$  structures and their electronic properties that are useful for various postfunctionalization applications.

We have developed a simple and general approach to noncovalent functionalization and subsequent immobilization of various biological molecules onto nanotubes.<sup>52</sup> The noncovalent scheme involves  $\pi$ -stacking of 1-pyrenebutanoic acid succinimidyl ester onto the sidewalls of SWNTs (Figure 10a). The anchored pyrene moieties on SWNTs are highly stable against desorption in aqueous solutions, leading to functionalization of SWNTs with succinimidyl ester groups. The mechanism of protein immobilization on nanotubes, then, involves the nucleophilic substitution of *N*-hydroxysuccinimide by an amine group on the protein, resulting in the formation of an amide bond. This technique has enabled the immobilization of a wide range of biomolecules on the sidewalls of SWNTs with high efficiency, as demonstrated with ferritin (Figure 10b), streptavidin, and biotin-PEO-amine.<sup>52</sup>

Nanotube functionalization and bioimmobilization are motivated by the recent activities in biological applications of novel solid-state nanomaterials. The unique physical properties of molecular-scale or nanoscale solids (dots or wires), when utilized in conjunction with the remarkable biomolecular recognition capabilities, could lead to miniature biological electronic devices, including probes and sensors. The interface between biological molecules and nanomaterials is critical to such applications. With nanotubes, such exploration is still in its early stage, with wide-open room and many possibilities.

## Summary

This Account has presented our work from controlling the synthesis of carbon nanotubes to using them as model systems for nanoscale science. The topics range from materials chemistry, solid-state physics, and surface chemistry/photochemistry to biological aspects of nanomaterials. As the synthesis–characterization–application cycle continues for nanotubes, gaining further control over their synthesis will remain at the heart of our research. Further exciting developments in nanoscale science and technology are expected.

*This work was carried out by a group of outstanding students and postdoctoral fellows. We have greatly enjoyed collaborations with Professors C. Quate, S. Fan, S. Y. Wu, C. S. Jayanthi, K. Cho, S. Manalis, C. Marcus, and R. Laughlin. This work has been supported by NSF, DARPA, SRC, the Packard Foundation, the Sloan Foundation, ABB, a Terman Fellowship, NSF/NNUN, LAM (Stanford), the Camille Henry Dreyfus Foundation, and the ACS-PRF.*

## References

- (1) Dresselhaus, M. S.; Dresselhaus, G.; Eklund, P. C. *Science of Fullerenes and Carbon Nanotubes*; Academic Press: San Diego, 1996; p 985.
- (2) Dresselhaus, M. S.; Dresselhaus, G.; Avouris, P. Carbon Nanotubes. In *Topics in Applied Physics*; Springer: Berlin, 2001.
- (3) Dekker, C. Carbon nanotubes as molecular quantum wires. *Phys. Today* **1999**, *52*, 22–28.
- (4) McEuen, P. L. Single-wall carbon nanotubes. *Phys. World* **2000**, *13* (6), 31–36.
- (5) Dai, H. Controlling nanotube growth. *Phys. World* **2000**, *13* (6), 43–47.
- (6) Dai, H. Nanotube Growth and Characterization. *Carbon Nanotubes*; Springer: Berlin, 2001; pp 29–53.
- (7) Liang, W.; Bockrath, M.; Bozovic, D.; Hafner, J.; Tinkham, M.; et al. Fabry–Perot interference in a nanotube electron waveguide. *Nature* **2001**, *411*, 665–669.
- (8) Kong, J.; Yenilmez, E.; Tombler, T. W.; Kim, W.; Liu, L.; et al. Quantum interference and ballistic transmission in nanotube electron waveguides. *Phys. Rev. Lett.* **2001**, *87*, 106801.
- (9) Kong, J.; Soh, H.; Cassell, A.; Quate, C. F.; Dai, H. Synthesis of individual single-walled carbon nanotubes on patterned silicon wafers. *Nature* **1998**, *395*, 878–881.
- (10) Hafner, J.; Bronikowski, M.; Azamian, B.; Nikolaev, P.; Colbert, D.; et al. Catalytic growth of single-wall carbon nanotubes from metal particles. *Chem. Phys. Lett.* **1998**, *296*, 195–202.
- (11) Satishkumar, B.; Govindaraj, A.; Sen, R.; Rao, C. Single-walled nanotubes by the pyrolysis of acetylene–organometallic mixtures. *Chem. Phys. Lett.* **1998**, *293*, 47–52.
- (12) Nikolaev, P.; Bronikowski, M. J.; Bradley, R. K.; Rohmund, F.; Colbert, D. T.; et al. Gas-phase catalytic growth of single-walled carbon nanotubes from carbon monoxide. *Chem. Phys. Lett.* **1999**, *313*, 91–97.
- (13) Su, M.; Zheng, B.; Liu, J. A scalable CVD method for the synthesis of single-walled carbon nanotubes with high catalyst productivity. *Chem. Phys. Lett.* **2000**, *322*, 321–326.

- (14) Colomer, J.-F.; Stephan, C.; Lefrant, S.; Tendeloo, G. V.; Willems, I.; et al. Large-scale synthesis of single-wall carbon nanotubes by catalytic chemical vapor deposition (CCVD) method. *Chem. Phys. Lett.* **2000**, *317*, 83–89.
- (15) Journet, C.; Maser, W. K.; Bernier, P.; Loiseau, A.; Delachapelle, M. L.; et al. Large-scale production of single-walled carbon nanotubes by the electric-arc technique. *Nature* **1997**, *388*, 756–758.
- (16) Thess, A.; Lee, R.; Nikolaev, P.; Dai, H. J.; Petit, P.; et al. Crystalline ropes of metallic carbon nanotubes. *Science* **1996**, *273*, 483–487.
- (17) Fan, S.; Chapline, M.; Franklin, N.; Tomblor, T.; Cassell, A.; et al. Self-oriented regular arrays of carbon nanotubes and their field emission properties. *Science* **1999**, *283*, 512–514.
- (18) Cassell, A.; Franklin, N.; Tomblor, T.; Chan, E.; Han, J.; et al. Directed growth of free-standing single-walled carbon nanotubes. *J. Am. Chem. Soc.* **1999**, *121*, 7975–7976.
- (19) Franklin, N.; Dai, H. An enhance chemical vapor deposition method to extensive single-walled nanotube networks with directionality. *Adv. Mater.* **2000**, *12*, 890–894.
- (20) Zhang, Y.; Chan, A.; Cao, J.; Wang, Q.; Kim, W.; et al. Electric-field-directed growth of aligned single-walled carbon nanotubes. *Appl. Phys. Lett.* **2001**, *79*, 3155–3157.
- (21) Li, Y.; Kim, W.; Zhang, Y.; Rolandi, M.; Wang, D.; et al. Growth of Single-Walled Carbon Nanotubes from Discrete Catalytic Nanoparticles of Various Sizes. *J. Phys. Chem. B* **2001**, *105*, 11424–11431.
- (22) Zhang, Y.; Li, Y.; Kim, W.; Wang, D.; Dai, H. Imaging as-grown single-walled carbon nanotubes originated from isolated catalytic nanoparticles. *Appl. Phys. A* **2002**, *74*, 325–328.
- (23) Li, Y.; Liu, J.; Wang, Y.; Wang, Z. L. Preparation of Monodispersed Fe–Mo Nanoparticles as the Catalyst for CVD Synthesis of Carbon Nanotubes. *Chem. Mater.* **2001**, *13*, 1008–1014.
- (24) Franklin, N. R.; Li, Y.; Chen, R. J.; Javey, A.; Dai, H. Patterned growth of single-walled carbon nanotubes on full 4-inch wafers. *Appl. Phys. Lett.* **2001**, *79*, 4571–4573.
- (25) Martel, R.; Schmidt, T.; Shea, H. R.; Hertel, T.; Avouris, P. Single- and multi-wall carbon nanotube field-effect transistors. *Appl. Phys. Lett.* **1998**, *73*, 2447–2449.
- (26) Zhou, C.; Kong, J.; Dai, H. Electrical measurements of individual semiconducting single-walled nanotubes of various diameters. *Appl. Phys. Lett.* **1999**, *76*, 1597–1599.
- (27) Derycke, V.; Martel, R.; Appenzeller, J.; Avouris, P. Carbon nanotube inter- and intramolecular logic gates. *Nano Lett.* **2001**, *1*, 453–456.
- (28) Bachtold, A.; Hadley, P.; Nakanishi, T.; Dekker, C. Logic circuits with carbon nanotube transistors. *Science* **2001**, *294*, 1317–1320.
- (29) Liu, X.; Lee, C.; Zhou, C.; Han, J. Carbon nanotube field-effect inverters. *Appl. Phys. Lett.* **2001**, *79*, 3329–3331.
- (30) Kong, J.; Franklin, N.; Zhou, C.; Chapline, M.; Peng, S.; et al. Nanotube molecular wires as chemical sensors. *Science* **2000**, *287*, 622–625.
- (31) Collins, P. G.; Bradley, K.; Ishigami, M.; Zettl, A. Extreme oxygen sensitivity of electronic properties of carbon nanotubes. *Science* **2000**, *287*, 1801–1804.
- (32) Sumanasekera, G.; Adu, C.; Fang, S.; Eklund, P. Effects of gas adsorption and collisions on electrical transport in single-walled carbon nanotubes. *Phys. Rev. Lett.* **2000**, *85*, 1096–1099.
- (33) Chen, R.; Franklin, N.; Kong, J.; Cao, J.; Tomblor, T.; et al. Molecular Photo-desorption from Carbon Nanotubes. *Appl. Phys. Lett.* **2001**, *79*, 2258–2260.
- (34) Zhou, C.; Kong, J.; Dai, H. Intrinsic electrical properties of single-walled carbon nanotubes with small band gaps. *Phys. Rev. Lett.* **2000**, *84*, 5604–5607.
- (35) Hamada, N.; Sawada, S.-i.; Oshiyama, A. New One-Dimensional Conductors: Graphitic Microtubules. *Phys. Rev. Lett.* **1992**, *68*, 1579–1581.
- (36) Blase, X.; Benedict, L. X.; Shirley, E. L.; Louie, S. G. Hybridization effects and metallicity in small radius carbon nanotubes. *Phys. Rev. Lett.* **1994**, *72*, 1878–1881.
- (37) Tomblor, T.; Zhou, C.; Alexeyev, L.; Kong, J.; Dai, H.; et al. Reversible Nanotube Electro-mechanical Characteristics Under Local Probe Manipulation. *Nature* **2000**, *405*, 769–772.
- (38) Liu, W.; Jayanthi, C.; Tang, M.; Wu, S. Y.; Tomblor, T.; et al. Controllable reversibility of an sp<sup>2</sup> to sp<sup>3</sup> transition of a single wall nanotube under the manipulation of an AFM tip: A nanoscale electromechanical switch? *Phys. Rev. Lett.* **2000**, *84*, 4950–4953.
- (39) Chang, H.; Lee, J.; Lee, S.; Lee, Y. Adsorption of NH<sub>3</sub> and NO<sub>2</sub> molecules on carbon nanotubes. *Appl. Phys. Lett.* **2001**, *79*, 3863–3865.
- (40) Peng, S.; Cho, K. Chemical control of nanotube electronics. *Nanotechnology* **2000**, *11*, 57–60.
- (41) Jhi, S.-H.; Louie, S. G.; Cohen, M. L. Electronic properties of oxidized carbon nanotubes. *Phys. Rev. Lett.* **2000**, *85*, 1710–1713.
- (42) Kittel, C. *Quantum Theory of Solids*; Wiley: New York, 1963.
- (43) Shim, M.; Javey, A.; Kam, N. W. S.; Dai, H. Polymer functionalization for air-stable n-type carbon nanotube field-effect transistors. *J. Am. Chem. Soc.* **2001**, *123*, 11512–11513.
- (44) Zhou, C.; Kong, J.; Yenilmez, E.; Dai, H. Modulated chemical doping of individual carbon nanotubes. *Science* **2000**, *290*, 1552–1555.
- (45) Kong, J.; Dai, H. Full and modulated chemical gating of individual carbon nanotubes by organic amine compounds. *J. Phys. Chem. B* **2001**, *105*, 2890–2893.
- (46) Kong, J.; Cao, J.; Dai, H.; Anderson, E. Chemical profiling of single nanotubes: intramolecular p–n–p junctions and on-tube single-electron transistors. *Appl. Phys. Lett.* **2002**, *80*, 73–75.
- (47) Grabert, H.; Devoret, M. H. *Single Charge Tunneling*; Plenum: New York, 1992.
- (48) Chen, J.; Hammon, M. A.; Hu, H.; Chen, Y. S.; Rao, A. M.; et al. Solution properties of single walled carbon nanotubes. *Science* **1998**, *282*, 95–98.
- (49) Boul, P.; Liu, J.; Mickelson, E.; Huffman, C.; Ericson, L.; et al. Reversible sidewall functionalization of buckytubes. *Chem. Phys. Lett.* **1999**, *310*, 367–372.
- (50) Star, A.; Stoddart, J.; Steuerman, D.; Diehl, M.; Boukai, A.; et al. Preparation and properties of polymer-wrapped single-walled carbon nanotubes. *Angew. Chem., Int. Ed.* **2001**, *40*, 1721–1725.
- (51) O'Connell, M. J.; Boul, P.; Ericson, L. M.; Huffman, C.; Wang, Y.; et al. Reversible water-solubilization of single-walled carbon nanotubes by polymer wrapping. *Chem. Phys. Lett.* **2001**, *342*, 265–271.
- (52) Chen, R.; Zhang, Y.; Wang, D.; Dai, H. Non-covalent sidewall functionalization of single-walled carbon nanotubes for protein immobilization. *J. Am. Chem. Soc.* **2001**, *123*, 3838–3839.

AR0101640